Polymer 54 (2013) 1218–1226

Contents lists available at SciVerse ScienceDirect

Polymer

journal homepage: www.elsevier.com/locate/polymer

Percolation and gel-like behavior of multiwalled carbon nanotube/polypropylene composites influenced by nanotube aspect ratio

Yongzheng Pan, Lin Li*

School of Mechanical and Aerospace Engineering, Nanyang Technological University, 50 Nanyang Avenue, Singapore 639798, Singapore

ARTICLE INFO

Article history:
Received 14 June 2012
Received in revised form
28 November 2012
Accepted 21 December 2012
Available online 2 January 2013

Keywords:
Polymer composite
Gel-like behavior
Percolation

ABSTRACT

The influence of aspect ratio of multiwalled carbon nanotube (MWCNTs) on rheological and electrical properties of MWCNT/polypropylene (PP) composites has been studied. Owing to the pre-grinding for MWCNTs and the efficient twin-extruder mixing, the dispersion of MWCNTs of different aspect ratios in the PP matrix is all uniform and homogeneous. With incorporation of 10 wt% MWCNTs with an aspect ratio of 167, an electrical conductivity of 1.2 S/cm could be achieved. A concept of "gel-like behavior" is introduced to investigate the MWCNT network formation within the composites. The rheological percolation threshold ($c_{pG'}$) and the gel content (c_g) of different MWCNT/PP composites are derived by applying the power law scaling and the Winter–Chambon method, respectively. It is revealed that the composites containing MWCNTs with the largest aspect ratio have the lowest $c_{pG'}$ and c_g values. Furthermore, the electrical conductivities of composites are measured and the electrical percolation thresholds ($c_{p\sigma}$) are obtained. The difference in gel content among different aspect ratios as well as the difference between rheological and electrical percolation thresholds is discussed.

© 2012 Elsevier Ltd. All rights reserved.

1. Introduction

Electrically conductive polymer composites (CPCs) have attracted extensive research interest because of their wide applications in electronic, aerospace and military areas. Owing to the high electrical conductivity and large aspect ratio, multiwalled carbon nanotubes (MWCNTs) are able to form an interconnected network throughout a polymer matrix at a low content, which promotes an effective transfer of their superior electrical properties to the matrix polymer, making them ideal nanofillers to fabricate CPCs. The CPCs show a sudden increase in electrical conductivity at a critical MWCNT content, which is generally referred to as the electrical percolation threshold. Recently, more and more efforts have been spent on fabricating MWCNT/polymer composites with lower percolation thresholds in a large scale via melt compounding for practical applications [1,2]. It has been known and found that the percolation threshold can be influenced by various factors including i) type [3], viscosity [4], and molecular weight [5] of a polymer matrix, ii) synthesis method [6], geometry [7], aspect ratio [8], and modification [9] of MWCNTs and iii) processing parameters like screw rate [10,11] and mixing time and temperature [12]. In short, any factor that affects the dispersion of MWCNTs and the formation of MWCNT network can influence the electrical percolation threshold. Therefore, it is of great importance to investigate the formation and density of MWCNT network for controlling the electrical performance of CPCs.

In addition to electrical characterization, dynamic rheological tests can also be employed to detect the MWCNT network in composites. With increasing MWCNT content in a composite, a composite melt undergoes a typical liquid-to-solid transition at low frequencies, indicating the emergence of an MWCNT network. The MWCNT content at which this transition occurs is defined as the rheological percolation threshold. A power law relation is generally used to determine the threshold of rheological percolation based on the values of storage modulus (G') [3,13–15]. The electrical percolation threshold can be estimated by measuring the rheological counterpart because both of them reflect the formation of an MWCNT network, though these two values are different, depending on the specific composite system. Bose et al. melt-mixed MWCNTs with 50/50 cocontinuous blends of polyamide 6 (PA6) and acrylonitrile–butadiene–styrene (ABS) and found that the electrical and rheological percolation thresholds were ~3–4 wt% and ~1–2 wt%, respectively [8]. McClory et al. studied the influence of screw speed on the electrical and rheological percolations of MWCNT/high-impact polystyrene (HIPS) composites. They revealed that the electrical percolation was located at ~1–3 wt% of

* Corresponding author. Tel.: +65 6790 6285; fax: +65 6791 1859.
E-mail address: mlli@ntu.edu.sg (L. Li).

0032-3861/$ – see front matter © 2012 Elsevier Ltd. All rights reserved.
http://dx.doi.org/10.1016/j.polymer.2012.12.058

LGES 1036
LGES v. MRD
IPR2024-01012

MWCNT at a screw speed of 100 rpm and increased to ~3–5 wt% when the screw speed was increased to 150 rpm [16]. The higher screw speeds (150 rpm) induced relatively higher shear forces on the molten composites, but the larger shear thinning effect within the extruder contributed to a more agglomerated MWCNT/HIPS morphology, leading to an increased electrical percolation.

On the other hand, the liquid-to-solid transition in a composite melt can also be considered as a physical gelling process [17]. Recently, some researchers studied the physical gelling behavior in CNT/polymer composites using the Winter–Chambon method [18–20], which is a classical method used to explore the characteristic of physical or chemical gels. As compared with the power law relation method, the Winter–Chambon method can not only accurately determine the gel content (c_g) but also quantitatively derive the gel strength S_g and exponent n, providing an effective way for detecting the MWCNT network and structure of composites. The gel content is supposed to be relevant to the rheological and electrical percolation thresholds, which may not be exactly the same. Therefore, it is interesting to further investigate the difference between gel content and percolation threshold, as well as their relationship with the MWCNT network formed in a polymer matrix.

We have previously studied the influence of MWCNT modification and melt annealing on the electrical properties of MWCNT/polypropylene (PP) composites [9,21]. In this study, we prepared MWCNT/PP composites containing MWCNTs with different aspect ratios by melt mixing. The influence of the aspect ratio of MWCNT on the rheological percolation and gel-like behavior was examined. The power law scaling and Winter–Chambon method were employed to determine the rheological percolation thresholds and gel contents of the composites respectively. Then, the electrical properties of the composites were measured and the electrical percolation thresholds were compared with the rheological percolation thresholds and gel contents.

2. Experimental

2.1. Materials

Isotactic PP (M = 190,000) from Sigma–Aldrich (USA) with a density of 0.9 g/cm^3 was used as the matrix. Three different types of multi-wall carbon nanotubes (MWCNTs) with different aspect ratios were used. The first type of MWCNTs, purchased from Cheap Tubes Inc (USA), had the outer diameter of 8–15 nm and length of 10–50 μm. The second one was purchased from Iljin Nano Tech (Korea), and had the outer diameter of 10–15 nm and length of 10–20 μm. The third one (outer diameter of 5–20 nm and length of 1–10 μm) was purchased from Bayer Material Science AG. Sodium dodecylbenzene sulfonate (SDBS) was purchased from Fluka.

2.2. Preparation of composites

All the MWCNTs were ground into fine powder using an agate mortar and then dried at 80 °C for 12 h before use. For melt mixing, PP was first added into a counter-rotating twin-screw microcompounder (Haake MiniLab) at 200 °C, and then MWCNTs were gradually added into the PP melt. After adding all MWCNTs, the mixture was mixed at 50 rpm for 15 min. Then, the mixed MWCNT/PP composites were injection molded at 200 °C using a mini injection machine (Haake MiniJet), into test samples with a square sheet dimension of 20 mm side length and 1 mm thickness. Before tests, all the molded samples were annealed at 200 °C for 30 min in an oven with N_2 as purge gas.

2.3. Characterization

The length and diameter of the MWCNTs after mixing with PP were measured using a transmission electron microscope (TEM, JEOL JEM-2010). A certain amount of MWCNT/PP composites was heated up to 600 °C under nitrogen purge to remove the PP matrix, and then the residual MWCNTs were obtained. Approximately 2 mg of MWCNTs were dispersed into 20 ml of 0.1 wt% SDBS aqueous solution by a bath sonication for 5 min. Several drops of this dispersion were dripped onto a copper grid and dried naturally. MWCNTs remaining on the copper grid were observed under TEM. The magnifications used were 10,000–15,000 times, and 150 lengths were measured for each sample of MWCNTs. The morphological characterization of the composites was carried out using field emission scanning electron microscopy (FESEM, JEOL JSM-6700F). Samples were fractured in liquid nitrogen, and sputtered with gold before observation. Rheological measurements were performed on a rotational rheometer (ARES) with the molded samples (Φ25 mm × 1 mm). A parallel plate geometry (25 mm diameter) with a gap of 1 mm was used. In a dynamic frequency sweep from 0.1 to 100 rad/s at a proper strain within the linear viscoelastic region, the storage modulus G′, loss modulus G″ and complex viscosity η^* were measured at 200 °C for the different composites. Through-plane electrical conductivity of the composites was measured in accordance with ASTM D4496. Samples with a known cross-sectional area and thickness were placed between two copper electrodes and the direct current (DC) resistance was measured using a Fluke 110 multimeter. The surfaces of the sample in contact with the electrodes were covered with carbon paper in order to reduce errors in conductivity measurement due to microroughness of sample surfaces. It was ensured that the surface area of the electrodes exceeded the cross-sectional area of the samples. The lowest limit of the measurement was 1×10^{-9} S/cm.

3. Results and discussion

3.1. Aspect ratio and dispersion state of MWCNTs

The aspect ratio of an individual CNT is the ratio of its length to diameter, which is an important parameter affecting the properties of a polymer composite filled CNTs. In order to evaluate the real value of MWCNT aspect ratio, the MWCNTs embedded in the composites were collected by completely removing the polymer in the composites at 600 °C in nitrogen [21,22]. The diameters and lengths of three types of MWCNTs were measured under TEM observation and average values were obtained based on 150 measurements. Then the aspect ratios of the MWCNTs were calculated. Fig. 1 displays the histograms of length distribution of MWCNTs. The representative TEM images of different MWCNTs are shown in Fig. 2. The diameters of three kinds of MWCNTs were within a similar range and their different lengths led to distinct aspect ratios, as summarized in Table 1. In the following discussion, three MWCNTs are named in terms of their respective aspect ratio, e.g. MWCNT51, MWCNT84 and MWCNT167.

Since a uniform and homogeneous dispersion of nanotubes in the matrix is crucial to the macroscopic properties of the composites, the dispersion state of nanotubes in these composites was examined by observing the fractured surfaces of the composites using FESEM. A set of FESEM images of different MWCNT/PP composites containing 3 wt% MWCNTs under different magnifications are shown in Fig. 3. It is clearly observed that, for all three different MWCNT/PP composites, most of MWCNTs are homogeneously dispersed in the PP matrix with a small amount of loose aggregates only. We believe that the loose aggregates would take a trivial effect on composite properties as compared with the large amount of dispersed nanotubes. From the

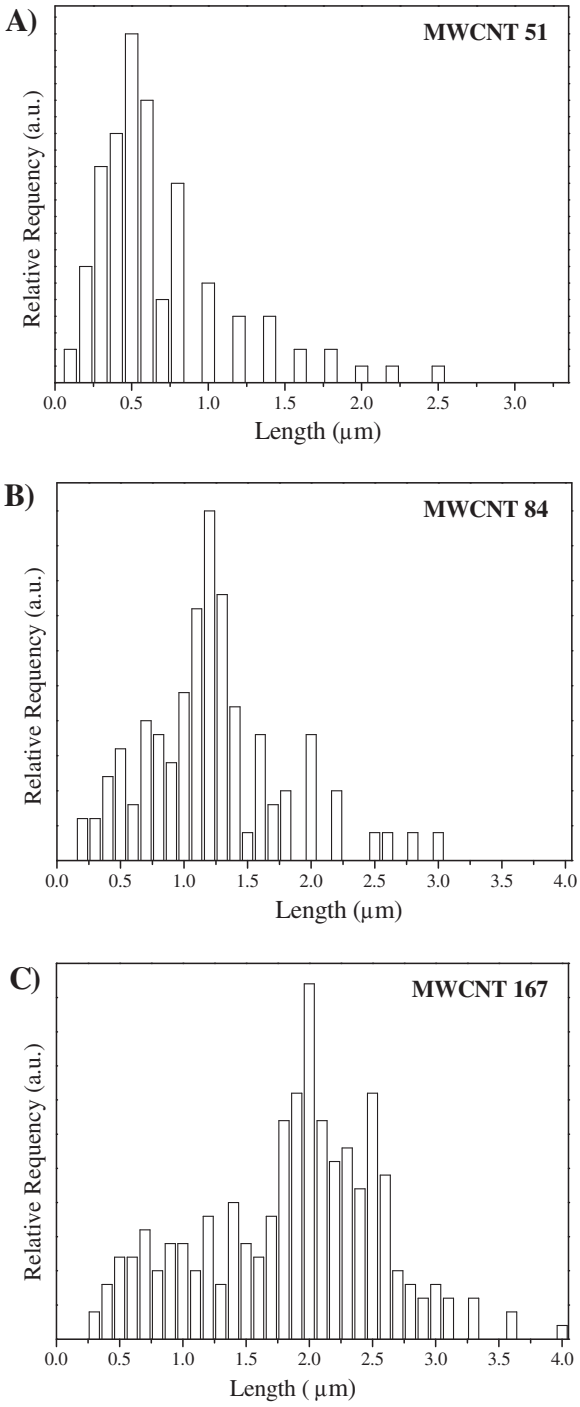


Fig. 1. Length distribution of different MWCNTs: (A) MWCNT51, (B) MWCNT84 and (C) MWCNT167.

images of a low magnification (×10,000, A1, B1 and C1), it is observed that the dispersion state of the pristine MWCNT51 in the PP matrix is better than that in our previous work [9,21], which should be attributed to the pre-grinding of MWCNTs before melt mixing. From the images at the high magnification (×30,000, A2, B2 and C2), we clearly observe the partially pulled out and broken MWCNT segments which were formed during fracture. However, it is hard to view the differences in the length among MWCNTs with different aspect ratios from the FESEM images because most of the MWCNTs were embedded in the PP matrix.

3.2. Rheological behavior of the MWCNT/PP composites

Dynamic rheological analysis is widely used to investigate polymer blends and polymer composites. The rheological characterization of different MWCNT/PP composites was carried out with the aim to elucidate the influence of MWCNT contents and aspect ratio on the formation of an MWCNT network. Fig. 4 and fig S1 in Supporting Information show the variation of storage modulus (G') and loss modulus (G'') as a function of angular frequency (ω) for different MWCNT/PP composites. Taking Fig. 4A and fig S1A as an example, at 200 °C and in the low ω zone, neat PP exhibits a typical terminal behavior, in which G' and G'' followed the scaling laws: $G' \sim \omega^1$ and $G'' \sim \omega^2$, due to full relaxation of PP chains. With addition of MWCNT51, both G' and G'' gradually increase in magnitude and showed a deviation from the terminal behavior, which gives rise to the appearance of a G' plateaus in the low ω zone, indicating the increased elastic response of the composites. As the content of MWCNT51 further increases, both G' and G'' become almost independent of ω at low ω, implying a transition from a liquid-like to solid-like viscoelastic behavior. This is because the long-range polymer chain relaxation in the composites was substantially constrained by the presence of MWCNTs. In contrast, MWCNTs did not influence short-range dynamics of the polymer chains significantly [13], accounting for the weakly affected rheological behavior at high ω. The other two composites reveal the similar evolution of G' and G'', but the deviation from the terminal behavior of each sample occurrs at different MWCNT contents.

Phase angle (δ) is quite sensitive to the liquid-to-solid transition for a heterogeneous polymeric system. Therefore, the van Gurp–Palmen plot is employed to study the structural changes of polymer composites, where the phase angle is plotted against the complex modulus ($|G^*|$). This method was used to roughly estimate the rheological percolation of the composites containing inorganic fillers in some previous reports [3,15,23]. Fig. 5 shows the van Gurp–Palmen plots for various samples. For neat PP which could completely relax at 200 °C, the value of δ is close to 90° in the low $|G^*|$ region. The deviation of δ from 90° in the high $|G^*|$ region suggests the elastic response of polymer chains, resulting from a network structure in the polymer melt. For MWCNT/PP composites, continuous descending of the δ versus $|G^*|$ curves with increasing MWCNT content is clearly observed, suggesting the increase of elastic portion of the composites. Further loading of MWCNTs results in the appearance of a δ maximum at a certain intermediate $|G^*|$ due to the formation of a pseudo-solid-like MWCNT network. For a heterogeneous composite system, the δ response above 45° suggests a viscous flow while that below 45° is indicative of an elastic one. In Fig. 5A and B, δ values of both MWCNT51/PP and MWCNT84/PP composites incipiently decrease below 45° with addition of 3 wt% MWCNT, indicating that the liquid-to-solid transitions probably occurred between 1 wt% and 3 wt% of MWCNT content, whereas this transition occurred between 0.5 wt% and 1 wt% for MWCNT167/PP composites (Fig. 5C). The van Gurp–Palmen plots demonstrate the approximate MWCNT content region where a liquid-to-solid transition occurs, and the estimated MWCNT contents for the transition are in fair agreement with those evaluated from G' curves discussed above (Fig. 4).

From the experimental results, it is known that after the MWCNT content reaches the so-called 'percolation threshold value', a stiff MWCNT 3D network will be formed to induce a sudden liquid-to-solid transition in the composites. To illustrate the influence of MWCNT aspect ratio on the rheological percolation behavior, we used a power law scaling method to attain the percolation values. At a fixed ω, a power law dependence of G' on the MWCNT content exists, which is near the percolation threshold in these composites.

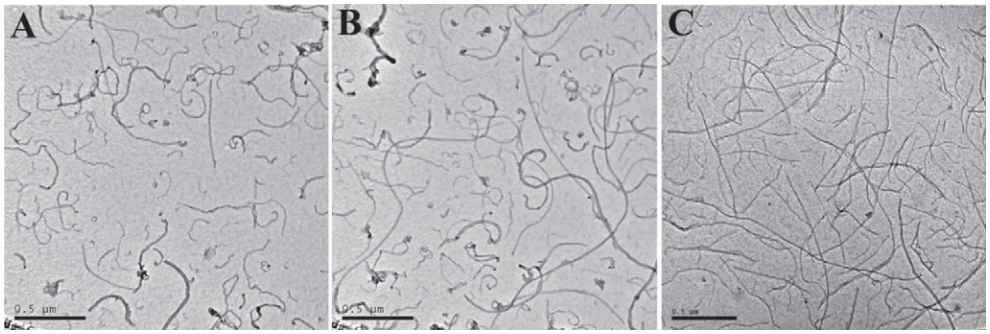


Fig. 2. TEM images of (A) MWCNT51, (B) MWCNT84 and (C) MWCNT167.

$$G' \propto \left(c - c_{pG'}\right)^{\beta'_G} \tag{1}$$

where G' is the storage modulus, c is the MWCNT mass fraction, $c_{pG'}$ is the threshold of the rheological percolation, and $\beta_{G'}$ is the critical exponent. Since G' is more sensitive in the low zone, the G' values at 0.5 rad/s of various MWNCT/PP composites were selected and plotted as a function of MWCNT content in Fig. 6A. An expected power law relationship between G' and $c-c_{pG'}$ at the onset of the rheological percolation is depicted in Fig. 6B and the determined percolation value and exponent for each composite are listed in Table 2. The percolation threshold values of MWCNT51, MWCNT84 and MWCNT167/PP composites are 1.64 wt%, 1.19 wt% and 0.35 wt %, respectively, suggesting that a higher MWCNT aspect ratio leads to a lower percolation value. The derived $\beta_{G'}$ values locate in a small range from 2.24 to 2.48, which seems to be irrelevant to the aspect ratio of MWCNTs. Indeed, $\beta_{G'} = 2$ is a typical experimental value for networks of stiff fibers [24]. The $\beta_{G'}$ values ranging from 1.5 to 3, which were obtained experimentally, have been reported for CNT/polymer composites [3,25]. $\beta_{G'}$ may be affected by the testing temperature and frequency.

With further increasing MWCNT content above the percolation threshold, a 3-D MWCNT network throughout the polymer matrix is gradually formed and becomes dense. We found that the formation and evolution of the MWCNT network in a polymer matrix was quite similar to a physical gel, like the typical physical gelling system, poly(vinyl chloride) (PVC)/dioctyl phthalate (DOP) [26], in which the formation of crystalline segments of PVC molecular chains was essential to construct a cross-linked network. The nanotube entanglement, van der Waals forces among nanotubes, and interaction between the polymer chains and nanotubes are possible factors responsible for the network formation in an MWCNT/PP composite. To study the gel-like behavior of MWCNT/PP composites and the influence of MWCNT aspect ratio, the well-established Winter and Chambon method is employed to analyze the rheological data and to derive the gel content (c_g), relaxation exponent (n) and gel strength (S_g) for each composite. Winter and Chambon experimentally found that the shear relaxation modulus of critical gels exhibited a simple power-law relaxation [27,28]:

$$G(t) = S_g t^{-n} \tag{2}$$

Table 1
Length, diameter and aspect ratio of various MWCNTs in MWCNT/PP composites.

Sample	Length (μm)	Diameter (nm)	Aspect ratio
MWCNT51	0.66 ± 0.11	13 ± 3	51
MWCNT84	1.23 ± 0.21	14 ± 2	84
MWCNT167	1.84 ± 0.37	11 ± 2	167

The gel strength and relaxation exponent characterize the critical gel. G' and G'' obey a generalized scaling law at the gel point:

$$G'(\omega) \sim G''(\omega) \sim \omega^n \quad 0 < n < 1 \tag{3}$$

or

$$\frac{G''(\omega)}{G'(\omega)} = \tan\delta = \tan\left(\frac{n\pi}{2}\right) \tag{4}$$

A system with n equal to 1 is regarded as a purely viscous gel, whereas n equal to 0 means a purely elastic gel. The characteristic frequency-independence of tan δ in the vicinity of the gel point has been widely proved for chemical and physical gels and used to determine the gel point [29]. Since the dynamic shear moduli G' and G'' are given by

$$G'(\omega) = \omega \int_0^\infty G(t)\sin(\omega t)dt \tag{5}$$

$$G''(\omega) = \omega \int_0^\infty G(t)\cos(\omega t)dt \tag{6}$$

the storage modulus and loss modulus scale with frequency at the gel point and the relationship are then expressed as follows

$$G'(\omega) = \frac{G''(\omega)}{\tan\left(\frac{n\pi}{2}\right)} = S_g \omega^n \Gamma(1-n)\cos\left(\frac{n\pi}{2}\right) \tag{7}$$

where $\Gamma(1-n)$ is the gamma function.

To determine the gel point, we have to observe a frequency-independent point of tan δ from a multifrequency plot of tan δ versus MWCNT content. Fig. 7 shows the plots for different MWCNT/PP composites at 200 °C. The general trend is a gradual decrease in tan δ with increasing MWCNT content. In each plot, all the curves pass through a common point at an MWCNT content, which is defined as the gel point. Apparently, the accurate determination of the gel point for each composite suggests that the Winter–Chambon method is applicable to heterogeneous composite systems. The c_g values, which can be read straightly from the abscissa of the convergence point, are 1.92 wt%, 1.34 wt% and 0.7 wt% for MWCNT51/PP, MWCNT84/PP and MWCNT167/PP composites, respectively. Given a gel point and the corresponded tan δ values, the relaxation exponent could be simply calculated using Equation (4). In general, they are related to the fractal dimension and reflect the degree of compactness of the network. A smaller n value states for the formation of a more elastic gel [26,30]. For example, the n values of most chemical gels were reported to be 0.56 [31], and 0.45–0.5

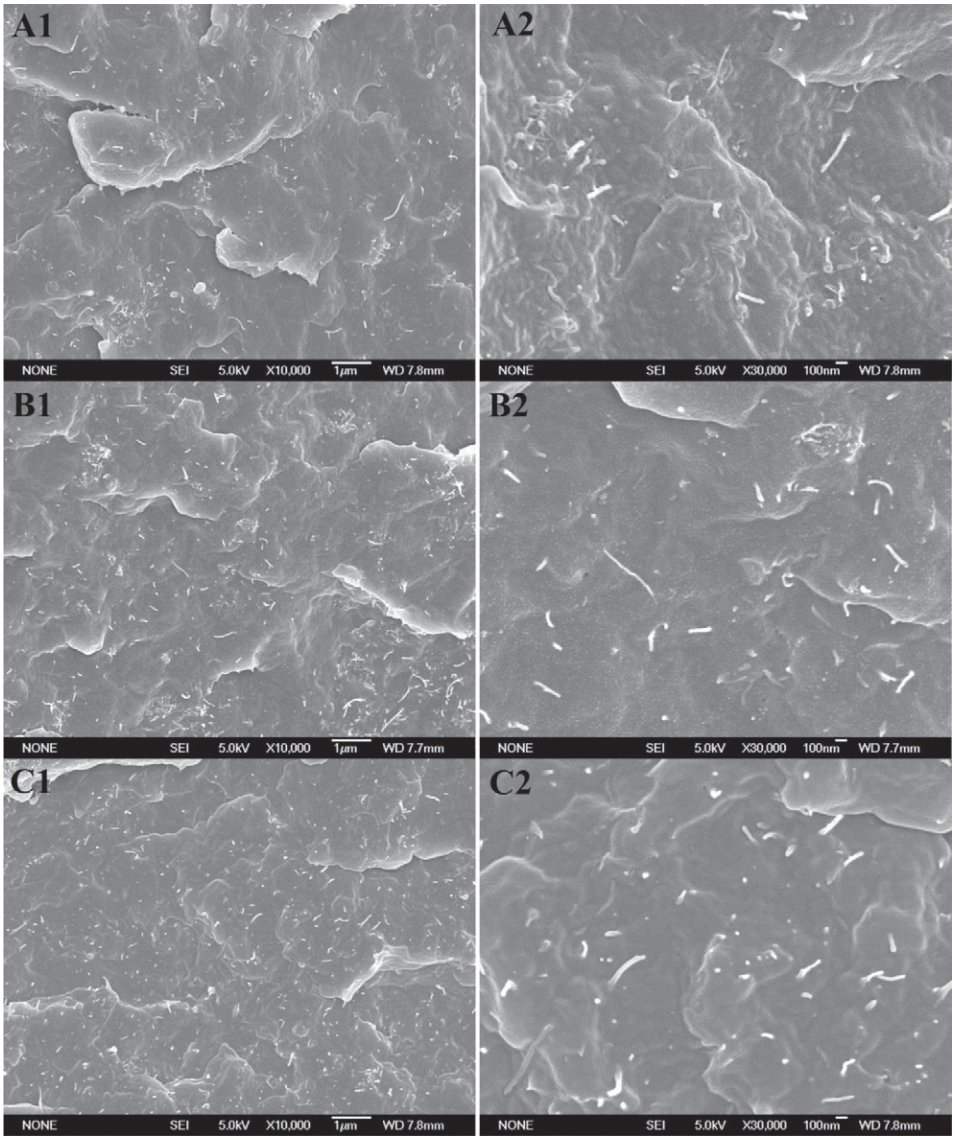


Fig. 3. FESEM images of different MWCNT/PP composites containing 3 wt% MWCNTs under different magnifications, (A) MWCNT51, (B) MWCNT84 and (C) MWCNT167.

[32], On the other hand, relatively big values of n were observed for the physical gels, whose gel strengths were relatively weak: 0.67–0.76 [29], 0.56–0.89 [26], 0.85–0.89 [33], and 0.56–0.89 [34]. The gel-like behavior of the MWCNT/PP composites originates from a combination of MWCNT entanglement and interaction between MWCNTs and polymer chains, both of which are physical interactions. Hence, the n values we obtained for the MWCNT/PP composites are comparable with those of the physical gelling systems.

The physical strength of a gelling system at the gel point can be described by gel strength defined by Equation (2). Although there is not a prepared sample exactly located at the gel point, we still can obtain the $G'(\omega)$ value at the gel point by plotting $G'(\omega)$ and $G''(\omega)$/tan $(n\pi/2)$ against MWCNT content, because the presence of a crossover of $G'(\omega)$ and $G''(\omega)$/tan $(n\pi/2)$ is certainly indicated by Equation (7). Fig. 8 shows an example of this plot for MWCNT167/PP composite, in which all crossover points appear at the gel point of $c_g = 0.7$ wt%, which is consistent with the value attained above (Fig. 7C). Using the G' value at any crossover point and Equation (7), S_g values were calculated to be 606 Pa s^n, regardless of which point of crossover was used. The S_g values of the other composites are listed in Table 2. Among these composites, MWCNT167/PP has the lowest n and the highest S_g values, approving that MWCNT167 performs better in enhancing the strength of the MWCNT network in the polymer matrix. Viewing from the theoretical simulations in the previous studies [35–37] for MWCNT/polymer systems, it is known that a percolation of nanotubes can be achieved with a large aspect ratio of CNTs at an extremely low content. A simulation done by Kyrylyuk et al. discovered that the percolation behavior of CNT/polymer system is very sensitive to the nanotubes with great lengths, and even small quantities of longer nanotubes lead to much lower percolation thresholds [35]. We revealed that the gel strength of MWCNT/PP at the gel point was also strongly related to the aspect ratio of MWCNTs, providing an insight view of this unique gel-like system. There are two dominant interactions when the composite system reaches the gel state. Firstly, the individually dispersed nanotubes may act as bridges among neighboring polymer random coils or crystalline zones so as to make formation of a network constructed by the polymer-MWCNT pairs. Secondly, nanotubes can entangle one another to develop an MWCNT network. Apparently, longer nanotubes are in favor of making the two interactions stronger, thus not only promoting the formation of an MWCNT network but also increasing its strength.

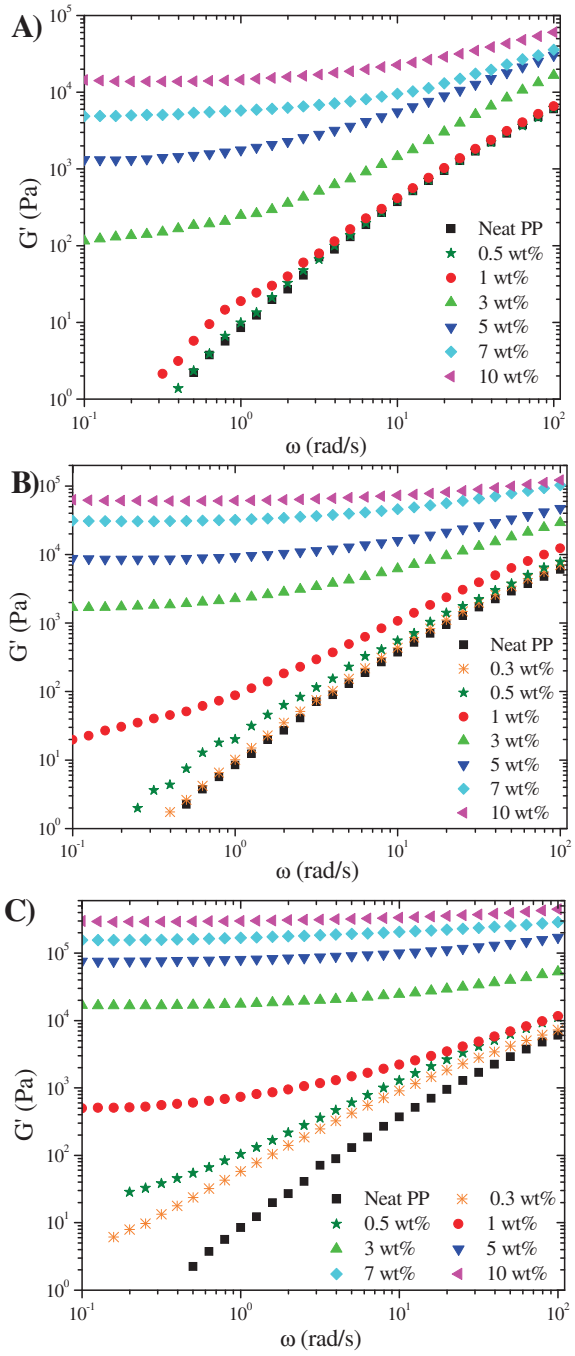


Fig. 4. Storage modulus (G') as a function of angular frequency (ω) for the composites containing various MWCNTs: (A) MWCNT51, (B) MWCNT84 and (C) MWCNT167.

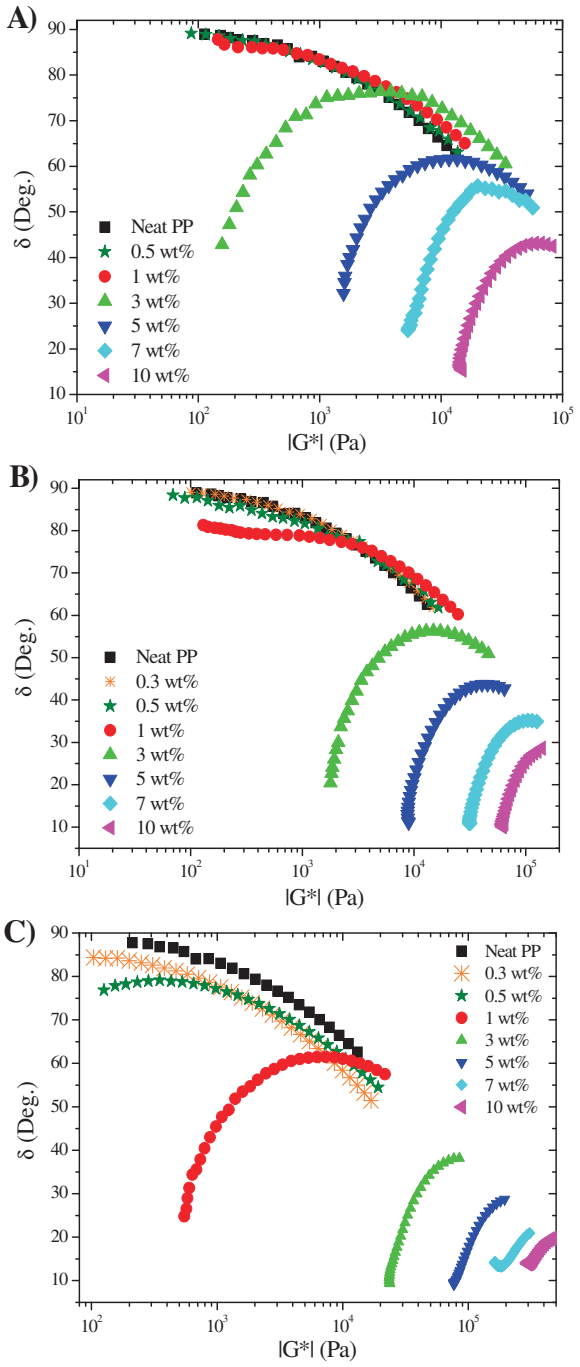


Fig. 5. Phase angle (δ) as a function of dynamic complex modulus ($|G^*|$) for the PP composites containing various MWCNTs: (A) MWCNT51/PP, (B) MWCNT84/PP and (C) MWCNT167/PP.

3.3. Electrical conductivity of MWCNT/PP composites

To further understand the influence of MWCNT aspect ratio on composite's structure and properties, we examined electrical conductivities of various MWCNT/PP composites. Our previous studies have proved that electrical conductivities of MWCNT/PP composites directly prepared by melt mixing and injection molding were relatively low due to the disruption of MWCNT connections. Annealing above melt temperature of the composites for a certain time could increase conductivities to equilibrium values [21]. Fig. 9A shows the electrical conductivities as a function of MWCNT content for three composites after annealing at 200 °C for 30 min. The electrical conductivities of the composites strongly depend on MWCNT content and aspect ratio. The MWCNT167/PP composites have electrical conductivities almost 60 times higher than those of MWCNT51/PP composites as the former nanotube has a 3.3 times larger aspect ratio than the latter one. Some studies have manifested that intrinsic electrical conductivities of MWCNTs also affect the electrical performance of composites. However, it is difficult for us to isolate MWCNTs into individual ones and measure their conductivity. In order to apart from the influence of intrinsic conductivities of MWCNTs, we evaluated the electrical conductivity

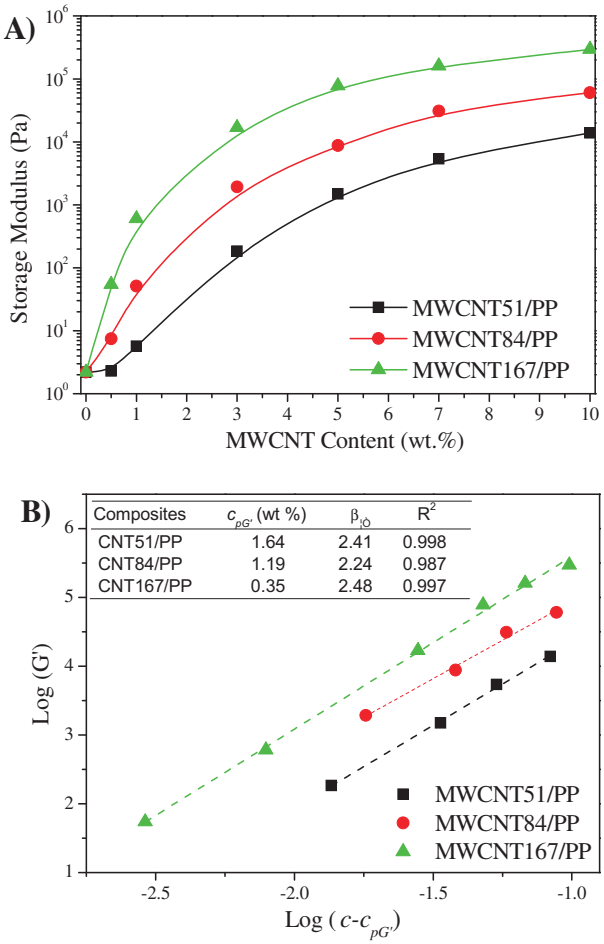


Fig. 6. (A) Storage modulus (G') at an angular frequency of 0.5 rad/s for the MWCNT/PP composites as a function of MWCNT content. (B) A log–log plot of G' versus reduced mass fraction. Inset is the percolation parameters of respective MWCNT/PP composites.

of MWCNTs indirectly by assessing their structural qualities via Raman spectroscopy, inspired by the relationship between structural defects and conductivities of MWCNTs [38]. fig S2 shows the Raman spectra of three kinds of MWNCTs. The disorder transition mode (D band) at around 1321 cm^{-1} and the characteristic tangential stretch mode (G band) at around 1573 cm^{-1} are observed for all MWNCTs. The I_D/I_G ratios of MWCNT51, MWCNT84 and MWCNT167 are 1.62, 1.49 and 1.58 respectively, which seem quite close, indicating the similar structural qualities of these MWCNTs. Therefore, it is believed the high electrical conductivity of MWCNT167/PP is mainly attributed to the dense conductive

Table 2
Rheological percolation and gel content parameters MWCNT/PP composites.

Composites	Rheological percolation[a]		Gel content[b]				
	(wt. %)	(vol. %)[c]	(wt. %)	(vol. %)[c]	Tan δ[d]	n[d]	S_g (Pa s^n)
MWCNT51/PP	1.64	0.85	1.92	0.99	6.01	0.895	233
MWCNT84/PP	1.19	0.61	1.34	0.69	3.28	0.812	467
MWCNT167/PP	0.35	0.18	0.70	0.36	2.30	0.740	606

[a] Obtained by power law scaling method.
[b] Obtained by Winter and Chambon method.
[c] Calculated using densities of 0.9 g/cm^3 for PP and 1.75 g/cm^3 for embedded MWCNTs.
[d] Tan δ and n values at gel content.

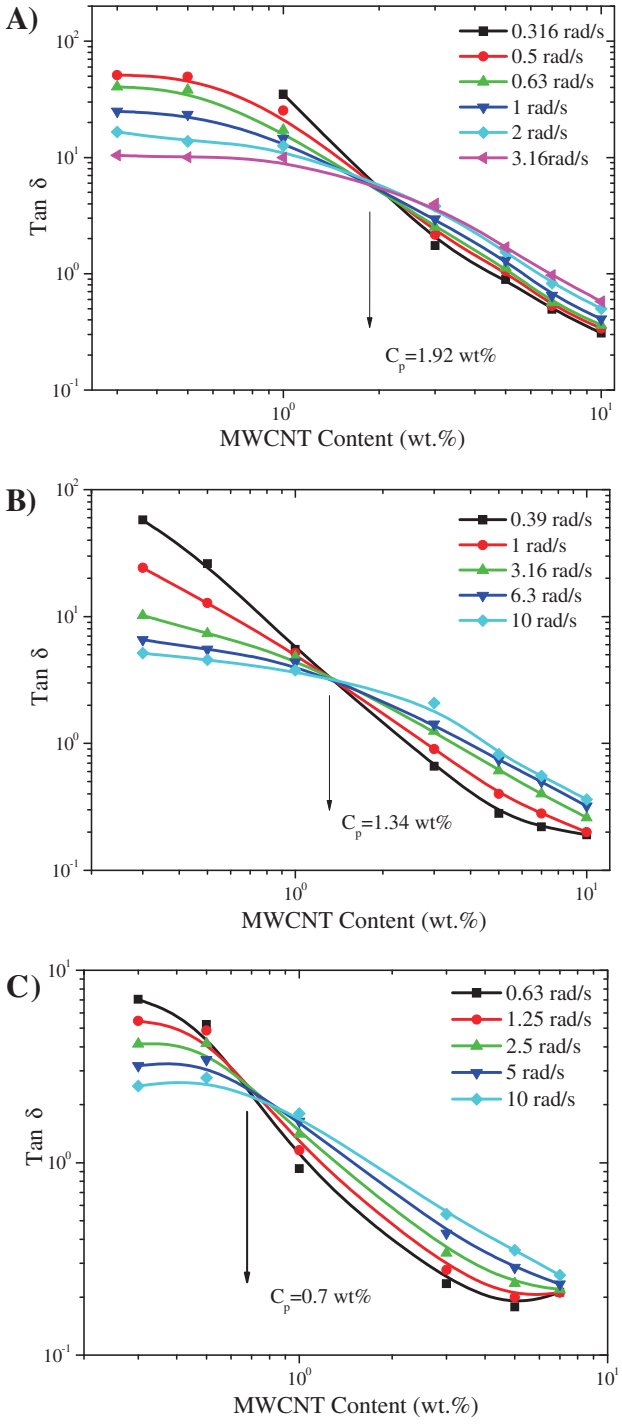


Fig. 7. Loss tangent (tan δ) as a function of MWCNT content for the PP composites containing various MWCNTs: (A) MWCNT51, (B) MWCNT84 and (C) MWCNT167. C_p is the MWCNT content at the gel point.

network resulted from the large aspect ratio of MWCNT167. Additionally, we reviewed electrical conductivities of MWCNT/PP composites reported in the recent literature and summarized these conductivities in Fig. 10. It is found that the maximum electrical conductivity of MWCNT/PP composites was 0.1 S/cm at 5 wt% [39]. The electrical conductivity of 1.2 S/cm at 10 wt% in this work is significantly higher than the previously reported values of MWCNT/PP composites [39–48].

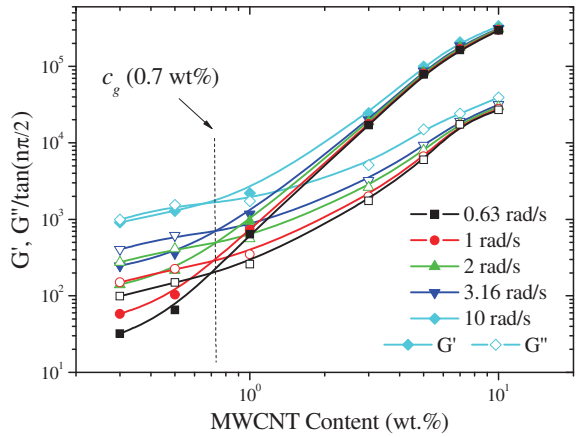


Fig. 8. Plots of G' and $G''/\tan(n\pi/2)$ versus MWCNT content for the MWCNT167/PP composites. The angular frequency was varied from 0.63 to 10 rad/s. $n = 0.74$ was used to calculate $G''/\tan(n\pi/2)$. The gel point is indicated by the arrow.

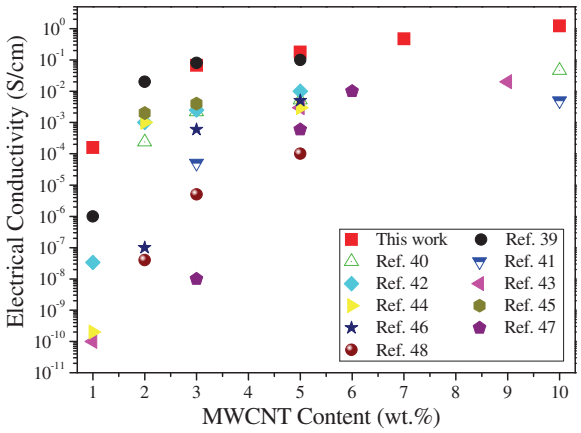


Fig. 10. Comparison of electrical conductivities with results in previous reports for MWCNT/PP composite systems [39–48].

In Fig. 9A, the three curves all show a typical percolation behavior. A power law relation is used to determine the electrical percolation threshold:

$$\sigma = (c - c_{p\sigma})^{\beta_\sigma} \tag{8}$$

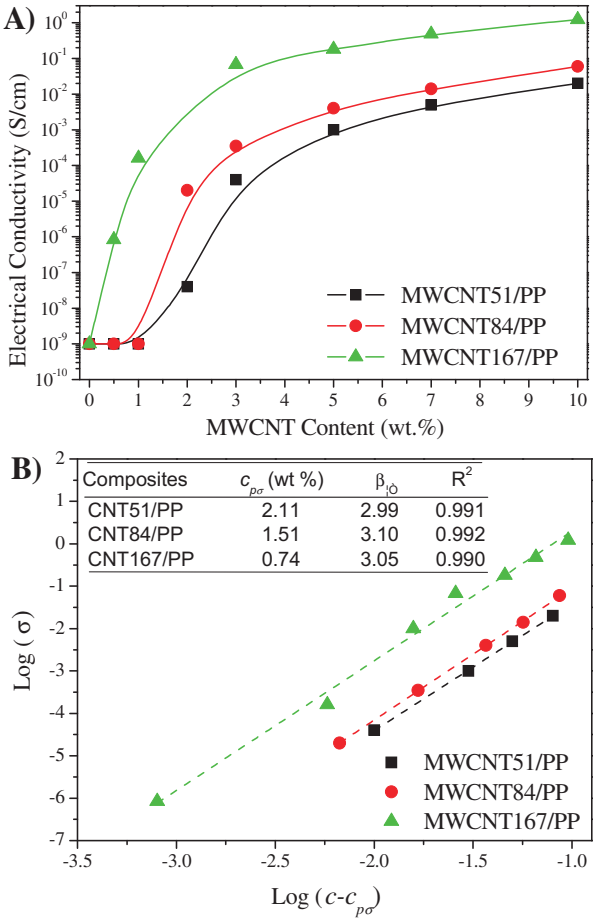


Fig. 9. (A) Electrical conductivity of the MWCNT/PP composites as a function of the MWCNT content. (B) A log–log plot of electrical conductivity versus reduced mass fraction. Inset is the percolation parameters for electrical properties of respective MWCNT/PP composites.

where σ is the electrical conductivity, c is the MWCNT mass content, $c_{p\sigma}$ is the percolation threshold of electrical conductivity, and β_σ is the critical exponent. The percolation parameters were determined by iteratively varying $c_{p\sigma}$, until the best linear fit of $\log\sigma$ versus $\log(c - c_{p\sigma})$ was obtained. Fig. 9B presents the percolation curves and the percolation parameters for the MWNCT/PP composites. Form the log–log plot, it is manifested that the scaling law is applicable for a very broad range of CNT content from 0.5 to 10 wt%. The $c_{p\sigma}$ values of these composites are 2.11 wt%, 1.51 wt% and 0.44 wt% for MWCNT51/PP, MWCNT84/PP and MWCNT167/PP composites, respectively. The obtained β_σ values seem to be independent of the nanotube's aspect ratio, and are within the range most often found for CNT/polymer composites [2].

To investigate the influence of MWCNT aspect ratio on rheological and electrical percolations, we compared these threshold values and gel contents with the theoretically estimated values. Theoretically, the percolation is related to the aspect ratio α of fillers. For randomly orientated ideal monodispersed penetrable rods with aspect ratios much larger than 1, the critical volume filler fraction for percolation can be well approximated by the following equation [35,49]:

$$\varphi_p = \frac{1}{2\alpha} \tag{9}$$

Considering the densities of 0.9 g/cm^3 for PP and 1.75 g/cm^3 for embedded MWCNTs, the relationship between α and CNT weight content (c_p) can be expressed as follows:

$$c_p = \frac{1.75\varphi_p}{1.75\varphi_p + 0.9\left(1 - \varphi_p\right)} = \frac{35}{36\alpha + 17} \tag{10}$$

The estimated percolation values by Equation (10) are plotted in Fig. 11, to compare with all the experimental values of the composites. It is shown that gel contents are higher than the rheological percolation values but lower than the electrical percolation values. The differences among these values should originate from the different stages of nanotube network formation. As we discussed above, the occurrence of rheological percolation is contributed from not only an MWCNT network but also a polymer-MWCNT network. When the distance between two nanotubes is smaller than the gyration radius of a polymer chain in the molten state (about dozens of nanometers), the nanotubes can be connected by random coils of polymer chains and restrict the polymer chain mobility [13,23,25]. As a result, rheological percolation can be achieved when a nanotube network is partially but not completely

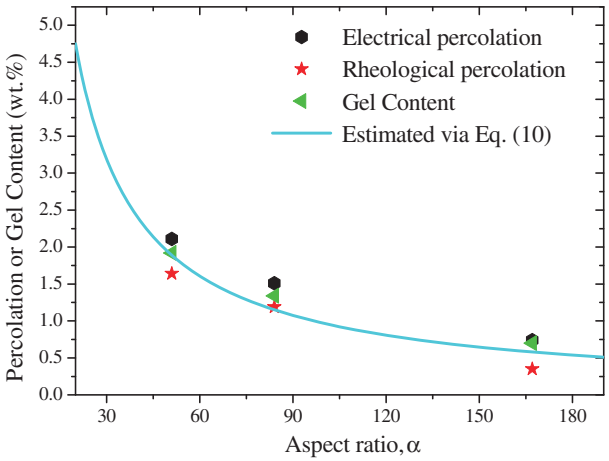


Fig. 11. Electrical percolation, rheological percolation, gel content values for MWCNT/PP composites and percolation values from estimation via Equation (10) as a function of aspect ratio.

constructed. In other words, it may correspond to a structure of MWCNT/PP composites with a nanotube network at the infant stage. Therefore, the lowest content of nanotubes is required to reach the rheological percolation. On the other hand, the gel contents resemble the geometrical percolation. At this stage, the MWCNT network become denser and the MWCNT/PP composites became more elastic. In the case of electrical percolation, only the MWCNT network contributes to emergence of conductance, so the network stems from nanotube network only. The nanotubes must directly contact with each other or locate within the distances smaller than the hopping distance of electrons, which is in the range of a few nanometers. Consequently, it requires more nanotubes to finally approach to the electrical percolation.

4. Conclusions

In summary, we fabricated MWCNT/PP composites containing three kinds of MWCNTs with different aspect ratios via melt mixing and studied the influence of MWCNT aspect ratio on percolation and gel-like behavior of the composites. FESEM confirmed that MWCNTs were dispersed uniformly and homogeneously in the PP matrix owing to the pre-grinding for MWCNTs and the efficiency of twin-extruder mixing. In order to detect the structure of composites and the formation of MWCNT network, we conducted the dynamic rheological measurements for the MWCNT/PP composites with different MWCNT contents. With increasing MWCNT content, the composites showed a typical transition from a liquid-like to a solid-like viscoelastic behavior. By utilizing the power law scaling and the Winter–Chambon method, the rheological percolation thresholds ($c_{pG'}$) and gel contents (c_g) of different composites were obtained, respectively. It was revealed that the composites containing MWCNTs with the largest aspect ratio had the lowest $c_{pG'}$ and c_g values. On the other hand, the electrical conductivities of composites were also tested and the electrical percolation thresholds ($c_{p\sigma}$) were obtained. Based on these results, the differences among gel content, rheological and electrical percolation thresholds were discussed and explained by the different stages of MWCNT network formation. Additionally, the incorporation of MWCNTs with larger aspect ratio could make composites have higher electrical conductivity in contrast to those with smaller aspect ratio MWCNTs. With addition of 10 wt% MWCNT167, an electrical conductivity of 1.2 S/cm could be achieved, which is higher than the values previously reported for the MWCNT/PP system.

Appendix A. Supplementary data

Supplementary data related to this article can be found at http://dx.doi.org/10.1016/j.polymer.2012.12.058.

References

[1] Alig I, Potschke P, Lellinger D, Skipa T, Pegel S, Kasaliwal GR, et al. Polymer 2012;53(1):4–28.
[2] Bauhofer W, Kovacs JZ. Compos Sci Technol 2007;69(10):1486–98.
[3] Huang CL, Wang C. Carbon 2011;49(7):2334–44.
[4] Socher R, Krause B, Muller MT, Boldt R, Potschke P. Polymer 2012;53(2):495–504.
[5] Kasaliwal GR, Goldel A, Potschke P, Heinrich G. Polymer 2011;52(4):1027–36.
[6] Krause B, Ritschel M, Taschner C, Oswald S, Gruner W, Leonhardt A, et al. Compos Sci Technol 2010;70(1):151–60.
[7] McClory C, McNally T, Baxendale M, Potschke P, Blau W, Ruether M. Eur Polym J 2010;46(5):854–68.
[8] Bose S, Bhattacharyya AR, Bondre AP, Kulkarni AR, Potschke P. J Polym Sci Part B: Polym Phys 2008;46(15):1619–31.
[9] Pan YZ, Li L, Chan SH, Zhao JH. Composites Part A 2010;41(3):419–26.
[10] Muller MT, Krause B, Kretzschmar B, Potschke P. Compos Sci Technol 2011;71(13):1535–42.
[11] Villmow T, Potschke P, Pegel S, Haussler L, Kretzschmar B. Polymer 2008;49(16):3500–9.
[12] Villmow T, Kretzschmar B, Potschke P. Compos Sci Technol 2010;70(14):2045–55.
[13] Du FM, Scogna RC, Zhou W, Brand S, Fischer JE, Winey KI. Macromolecules 2004;37(24):9048–55.
[14] Kayatin MJ, Davis VA. Macromolecules 2009;42(17):6624–32.
[15] Kota AK, Cipriano BH, Duesterberg MK, Gershon AL, Powell D, Raghavan SR, et al. Macromolecules 2007;40(20):7400–6.
[16] McClory C, Potschke P, McNally T. Macromol Mater Eng 2011;296(1):59–69.
[17] Potschke P, Abdel-Goad M, Alig I, Dudkin S, Lellinger D. Polymer 2004;45(26):8863–70.
[18] Park S-D, Han D-H, Teng D, Kwon Y. Curr Appl Phys 2008;8(3–4):482–5.
[19] Liu CY, Zhang J, He JS, Hu GH. Polymer 2003;44(24):7529–32.
[20] Huang SL, Liu ZY, Yin CL, Wang Y, Gao YJ, Chen C, et al. Macromol Mater Eng 2012;297(1):51–9.
[21] Pan YZ, Cheng HKF, Li L, Chan SH, Zhao JH, Juay YK. J Polym Sci Part B: Polym Phys 2010;48(21):2238–47.
[22] Fu SY, Chen ZK, Hong S, Han CC. Carbon 2009;47(14):3192–200.
[23] Menzer K, Krause B, Boldt R, Kretzschmar B, Weidisch R, Potschke P. Compos Sci Technol 2011;71(16):1936–43.
[24] Cipiriano BH, Kashiwagi T, Raghavan SR, Yang Y, Grulke EA, Yamamoto K, et al. Polymer 2007;48(20):6086–96.
[25] Hu G, Zhao C, Zhang S, Yang M, Wang Z. Polymer 2006;47(1):480–8.
[26] Li L, Aoki Y. Macromolecules 1997;30(25):7835–41.
[27] Chambon F, Winter HH. J Rheol 1987;31(8):683–97.
[28] Winter HH, Chambon F. J Rheol 1986;30(2):367–82.
[29] Sharma N, Kasi RM. Langmuir 2010;26(10):7418–24.
[30] Gao SJ, Nishinari K. Biomacromolecules 2004;5(1):175–85.
[31] Adzima BJ, Aguirre HA, Kloxin CJ, Scott TF, Bowman CN. Macromolecules 2008;41(23):9112–7.
[32] Mours M, Winter HH. Macromolecules 1996;29(22):7221–9.
[33] Lue A, Zhang L. Polymer 2010;51(12):2748–54.
[34] Wang YX, Lue A, Zhang LN. Polymer 2009;50(23):5474–81.
[35] Kyrylyuk AV, van der Schoot P. Proc Nat Acad Sci U S A 2008;105(24):8221–6.
[36] Balberg I, Anderson CH, Alexander S, Wagner N. Phys Rev B 1984;30(7):3933–43.
[37] Balberg I, Binenbaum N, Wagner N. Phys Rev Lett 1984;52(17):1465–8.
[38] Gomez-Navarro C, De Pablo PJ, Gomez-Herrero J, Biel B, Garcia-Vidal FJ, Rubio A, et al. Nat Mater 2005;4(7):534–9.
[39] Lee SH, Kim MW, Kim SH, Youn JR. Eur Polym J 2008;44(6):1620–30.
[40] Yang LB, Liu FH, Xia HS, Qian XY, Shen KZ, Zhang J. Carbon 2011;49(10):3274–83.
[41] Koval'chuk AA, Shchegolikhin AN, Shevchenko VG, Nedorezova PM, Klyamkina AN, Aladyshev AM. Macromolecules 2008;41(9):3149–56.
[42] Mičušík M, Omastová M, Krupa I, Prokeš J, Pissis P, Logakis E, et al. J Appl Polym Sci 2009;113(4):2536–51.
[43] Gorrasi G, Romeo V, Sannino D, Sarno M, Ciambelli P, Vittoria V, et al. Nanotechnology 2007;18(27):275703. 275701–275711.
[44] Seo MK, Park SJ. Chem Phys Lett 2004;395(1–3):44–8.
[45] Tjong SC, Liang GD, Bao SP. Scr Mater 2007;57(6):461–4.
[46] Lee SH, Cho E, Jeon SH, Youn JR. Carbon 2007;45(14):2810–22.
[47] Alig I, Lellinger D, Dudkin SM, Potschke P. Polymer 2007;48(4):1020–9.
[48] Logakis E, Pollatos E, Pandis C, Peoglos V, Zuburtikudis I, Delides CG, et al. Compos Sci Technol 2010;70(2):328–35.
[49] Castillo FY, Socher R, Krause B, Headrick R, Grady BP, Prada-Silvy R, et al. Polymer 2011;52(17):3835–45.